

Research on a Forest Fire Spread Simulation Driven by the Wind Field in Complex Terrain

Ying Shang, Chencheng Wang

Abstract—The wind field is the main driving factor for the spread of forest fires. For the simulation results of forest fire spread to be more accurate, it is necessary to obtain more detailed wind field data. Therefore, this paper studied the mountainous fine wind field simulation method coupled with WRF (Weather Research and Forecasting Model) and CFD (Computational Fluid Dynamics) to realize the numerical simulation of the wind field in a mountainous area with a scale of 30 m and a small measurement error. Local topographical changes have an important impact on the wind field. Based on the Rothermel fire spread model, a forest fire in Idaho in the western United States was simulated. The historical data proved that the simulation results had a good accuracy. They showed that the fire spread rate will decrease rapidly with time and then reach a steady state. After reaching a steady state, the fire spread growth area will not only be affected by the slope, but will also show a significant quadratic linear positive correlation with the wind speed change.

Keywords—Wind field, numerical simulation, forest fire spread, fire behavior model, complex terrain.

I. INTRODUCTION

A. Background and Significance of the Study

A terrestrial ecosystem is a complex ecosystem that includes many components such as plants, animals, microorganisms, soil, etc. on land. They have different division of labor, but interact with each other to form a stable system. Current research shows that forests are one of the largest and most important components of terrestrial ecosystems on Earth, playing a crucial role in maintaining ecological balance [1], [2]. They are also important for the survival and development of human beings. From both the perspective of forest protection and human development, it is of great significance to achieve more accurate forest fire spread simulation driven by wind fields in complex terrain. The factors affecting forest fire spread are known to be numerous and complex [3], [4], and the wind factor is the most important among the many meteorological factors that drive it. Accurate acquisition of meteorological wind fields is a prerequisite and decisive condition for forest fire spread prediction and emergency relief management and implementation [5], [6]. At present, although meteorological departments can provide monitoring and forecasting of wind fields on a regional scale, the wind fields obtained by site interpolation in mountainous areas where there are no stations are unable to accurately reflect the effects of terrain changes on wind fields, and cannot meet the needs of forest fire spread simulation. For this reason, numerical simulation methods are

becoming more and more important [7], [8].

Numerical simulation of wind fields is the main tool of current meteorological forecasting, and operates by solving a basic set of equations governing the atmospheric motion by means of numerical calculations with the aid of a computer, so as to simulate the state of atmospheric motion and its changes. For the simulation of small-scale fine wind fields in mountainous areas, research results offer useful information: Uchida et al. [9] studied the phenomenon of reattachment and flow separation in a mountainous terrain based on a large eddy simulation model. Griffiths et al. [10] used direct numerical simulation methods, as well as the RANS method, in the numerical simulation of wind fields in mountainous areas with differences in slope. In China, Zhang and Cheng [9] calculated the wind fields of wind farms in the Poyang Lake area and Yangmeishan wind farm area in Lu Liang County, Yunnan Province, by using the coupled WRF/Fluent model system. Chen [12] simulated the wind field characteristics of complex mountains with different incoming currents and wind directions, and the wind load body type of narrow-base angle steel transmission towers, using the Fluent model. Pan [13] used the Open FOAM open-source platform combined with the CFD numerical simulation model to simulate the wind field in the atmospheric boundary layer. Regarding the simulation of forest fire spread considering wind fields, Rothermel [14] proposed that the behavior of wildfires is strongly influenced by the wind speed and direction in the fire burning area. Butler et al. [15] demonstrated that accurate simulation of wind can improve the accuracy of fire behavior prediction. Herráez et al. [16] integrated a physical model of fire spread and a high-definition wind model (HDWM) into a GIS-based interface to simulate a real fire in Galicia, Spain. In China, Zhao et al. [17] implemented a forest fire spread simulation based on wind field interpolation in complex terrain.

In summary, the research on the simulation of forest fire spread driven by wind field in complex terrain is still in the initial stage, especially in China, and research on related methods and techniques is still limited. Frequent mountain forest fires in China have caused huge losses in recent years, and the research in this area needs to continue.

B. Research Content

To address the current problem of meteorological wind field uncertainty in mountain forest fire spread, this paper presents the mesoscale meteorological model—WRF Model [18], [19],

Ying Shang is with Chengdu University of Information Technology; Chengdu 610225, China (corresponding author, e-mail: shangyingwork@163.com).

Chencheng Wang is with Sichuan Province Meteorology Service; Chengdu 610072, China (e-mail: 3180205004@cuit.edu.cn).

nest the small-scale flow field numerical simulation model [20], parametrizes and localizes the model using multi-source meteorological data and multi-source remote sensing data, and simulates the local refined mountain wind field under the action of mountain topography and analyzes it. Then, it takes a former forest fire in Idaho as an example to provide more accurate meteorological conditions for the forest fire spread model by coupling with the fine wind field to realize the simulation of forest fire spread driven by fine wind field elements, and to determine the reasonableness of the simulation results by accuracy checking.

II. DATA AND METHODS

A. Research Area

Due to the specific topography and climate of Idaho in the western United States and the frequent occurrence of forest fires, a forest fire in Idaho was used as an example for this paper. Fig. 1 shows the geographical location and topographic overview of Idaho. The northern Rocky Mountains extend from the Canadian border to south-central Idaho and occupy more than half of the state, a region with many mountain ranges and undulating terrain. July and August are the hottest months of the year in Idaho, with average temperatures ranging from 26.1 °C to 35 °C and sunshine lasting up to 10 h per day. During this season, there is little to no precipitation in the north and west, and the hot and dry climate makes the region highly susceptible to forest fires during the summer [21], [22].

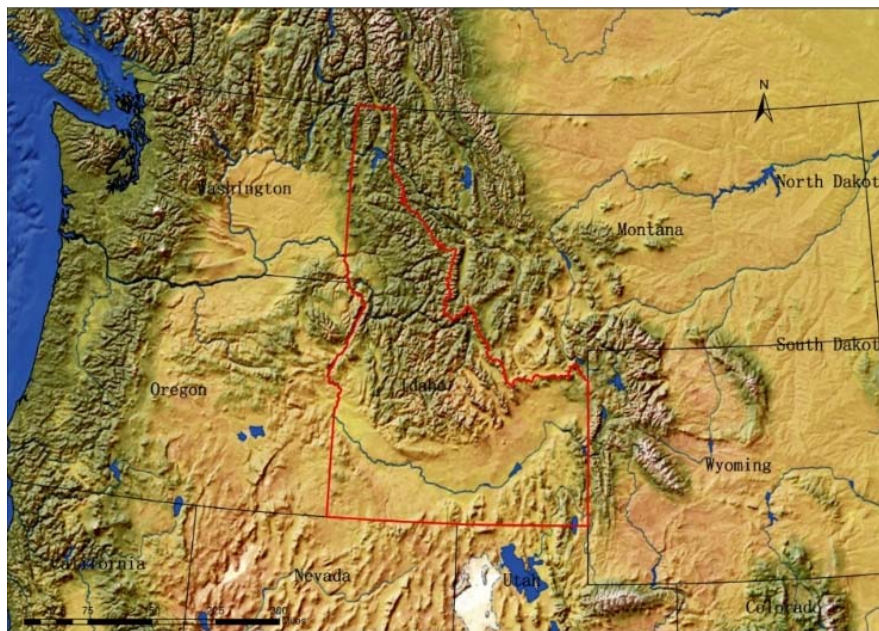


Fig. 1 Location and topographic profile of Idaho

TABLE I
 CONSTANTS USED IN THE GOVERNING EQUATION

Parameters	Standard k-e Equation	RNG k-e Equation
C_μ	0.09	0.085
σ_k	1.0	0.7179
σ_ε	1.3	0.7179
$C_{\varepsilon 1}$	1.44	Calculated values
$C_{\varepsilon 2}$	1.92	1.68
	--	0.012

B. Mathematical Foundations

1. Numerical Simulation Turbulence Model of the Wind Field

During the simulations in this study, the wind was used as a fluid and we assumed that its flow was steady incompressible turbulence. The Coriolis force was neglected and the turbulence

equations used the standard k-e model [23], [24] with:

$$\frac{\partial(k\bar{u}_i)}{\partial x_i} = \frac{\partial}{\partial x_j} \left[\frac{v_j}{\sigma_k} \frac{\partial k}{\partial x_j} \right] + P - \varepsilon \quad (1)$$

$$\frac{\partial(\varepsilon\bar{u}_i)}{\partial x_i} = \frac{\partial}{\partial x_j} \left[\frac{v_j}{\sigma_\varepsilon} \frac{\partial \varepsilon}{\partial x_j} \right] + C_{\varepsilon 1} \frac{P\varepsilon}{k} - C_{\varepsilon 2} \frac{\varepsilon^2}{k} \quad (2)$$

The constants used in the formula are shown in Table I.

2. Forest Fire Spread Simulation Base Model [25]-[27]

The base model for forest fire spread used in this study was the Rothermel model with the following spread equation:

$$R = \frac{I_R \xi (1 + \Phi_\omega + \Phi_s)}{\rho_b \varepsilon \phi_{ig}} \quad (1)$$

The units and meanings of the variables in the formula are shown in Table II.

TABLE II
 VARIABLES IN ROTHERMEL MODEL EQUATIONS AND THEIR MEANINGS

Component	Unit	Name	Explanation
R	ft/min	Rate of spread	Flaming front of a surface fire
I_R	Btu/ft ² /min	Reaction intensity	Energy release rate per unit area of fire front
ξ	dimensionless	Propagating flux ratio	Proportion of the reaction intensity that heats adjacent fuel particles to ignition (no wind)
ρ_b	lb/ft ³	Bulk density	Amount of oven-dry fuel per cubic foot of fuel bed
ε	dimensionless	Effective heating number	Proportion of a fuel particle that is heated to ignition temperature at the time flaming combustion starts
ϕ_{ig}	Btu/lb	Heat of preignition	Amount of heat required to ignite one pound of fuel
Φ_ω	dimensionless	Wind factor	Dimensionless multiplier that accounts for the effect of wind in increasing the propagating flux ratio
Φ_s	dimensionless	Slope factor	Dimensionless multiplier that accounts for the effect of slope in increasing the propagating flux ratio

C. Simulation Data Collection and Processing

The first part was the fine topographic data, including the 30 m digital elevation data of the study area, based on which the slope direction of the study area was obtained by pre-processing. The third part was the subsurface and boundary field data required for wind simulation, including surface type data, coarse resolution (1 km) topographic data, reanalysis data, etc. The last part was the fine meteorological station data, including temperature data, humidity data, precipitation data, cloud cover data, etc., in the study area.

D. Model Validation Methods

The data for the accuracy verification of the wind field simulations were selected from five remote automatic weather stations with no missing data within Custer County, Idaho, and the details are listed in Table III. The historical fire dataset provided by EROS and the USDA Forest Service Geospatial Technology and Applications Center (GTAC) records the location, time, and area of spread of all major fires in the United States from 1984 to the present. The accuracy validation parameters selected for this study were: root means square error (RMSE), mean absolute error (MAE), and the correlation coefficient (R).

TABLE III
 ACCURACY VERIFICATION OF THE REMOTE AUTOMATIC WEATHER STATION DETAILS

Station Number	Station Name	Long (°)	Lat (°)	Elevation (ft)
1	Bonanza	-114.340	44.223	6410
2	Challis	-114.132	44.302	5250
3	Little Creek	-114.540	44.300	4620
4	Red Rock Peak	-114.251	44.592	7910
5	Stanley	-114.553	44.101	6570

III. REFINEMENT OF MOUNTAIN WIND FIELD SIMULATION AND ANALYSIS

A. Accuracy Verification

In the wind simulation results, the average absolute error of the five sites was within a reasonable range, and the error direction angle did not exceed 10°. There was an anomaly in the analysis results; the correlation coefficient between the

simulated and real values of the wind direction angle at the Bonanza site was only -0.071. At the Bonanza site location, the direction change is complicated, and the historical real wind speed data recorded by the automatic site was susceptible to a variety of factors. The uncorrelated results within 24 h on 25 August are not representative.

TABLE IV
 ACCURACY VERIFICATION RESULTS OF WIND FIELD SIMULATION

Station name	Wind speed (m/s)			Wind direction angle (°)		
	MAE	RMSE	R	MAE	RMSE	R
Bonanza	1.879	4.851	0.807	9.511	132.788	-0.071
Challis	2.446	6.497	0.796	2.309	34.537	0.815
Little Creek	2.531	7.632	0.709	2.046	32.396	0.793
Red Rock Peak	2.962	10.810	0.931	3.958	27.479	0.858
Stanley	1.768	3.966	0.716	5.260	37.643	0.902

B. Influence of Topography on the Wind Field

Fig. 2 shows the results of the 30 m resolution wind speed simulation for the whole study area at 00:00 on 24 August against the mountainous terrain, and it can be seen from the figure that the variation of wind speed throughout the study area is highly correlated with the variation of mountainous terrain.

(1) Influence of valley topography on wind field variation.

As in Fig. 3, two valleys, (a) and (b), can be observed, and it is known that the dominant wind direction of the wind field in the region at this moment is approximately perpendicular to valley (a) and approximately parallel to valley (b). When the turbulent flow passes through valley (a), the wind direction is deflected and gradually aligns with the direction of valley (a), but the wind speed decreases to a certain extent, and the decrease is different at different locations; when the turbulent flow passes through valley (b), the flow speed increases significantly due to the inability of the airflow to accumulate, and the increase is different at different locations. The flow direction is consistent with the direction of the valley. When the wind field direction is parallel or nearly parallel to the valley direction, the wind direction through the valley will change due to the valley direction, and the wind speed will increase. The narrower the valley, the more obvious the increase in wind speed. When the wind field direction is perpendicular or nearly

perpendicular to the valley direction, the wind flow through the valley will also change due to the valley direction, and the speed

decreases when it reaches the valley area. The steeper the valley, the more obvious the deceleration.

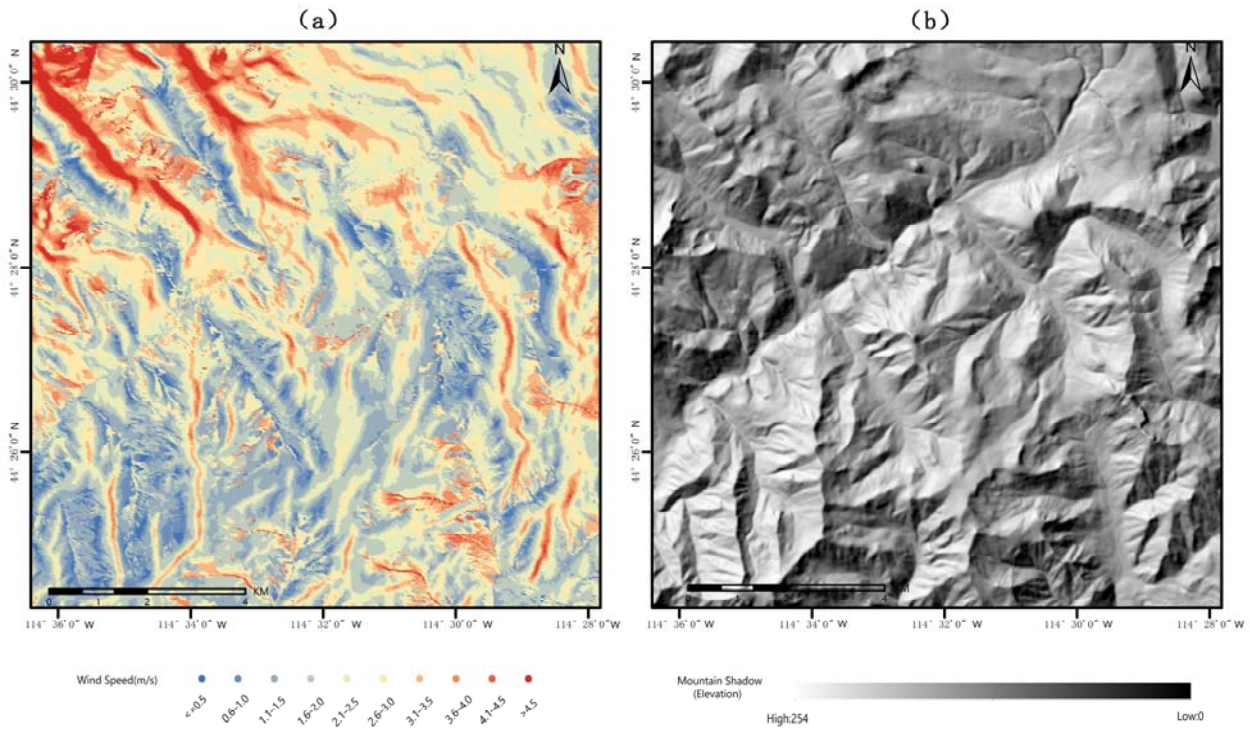


Fig. 2 Simulation results of wind speed in the study area with mountainous terrain at 00:00 on 24 August: (a) Simulation results of the 30 m wind field in the study area; (b) Topographic mountain shading in the study area

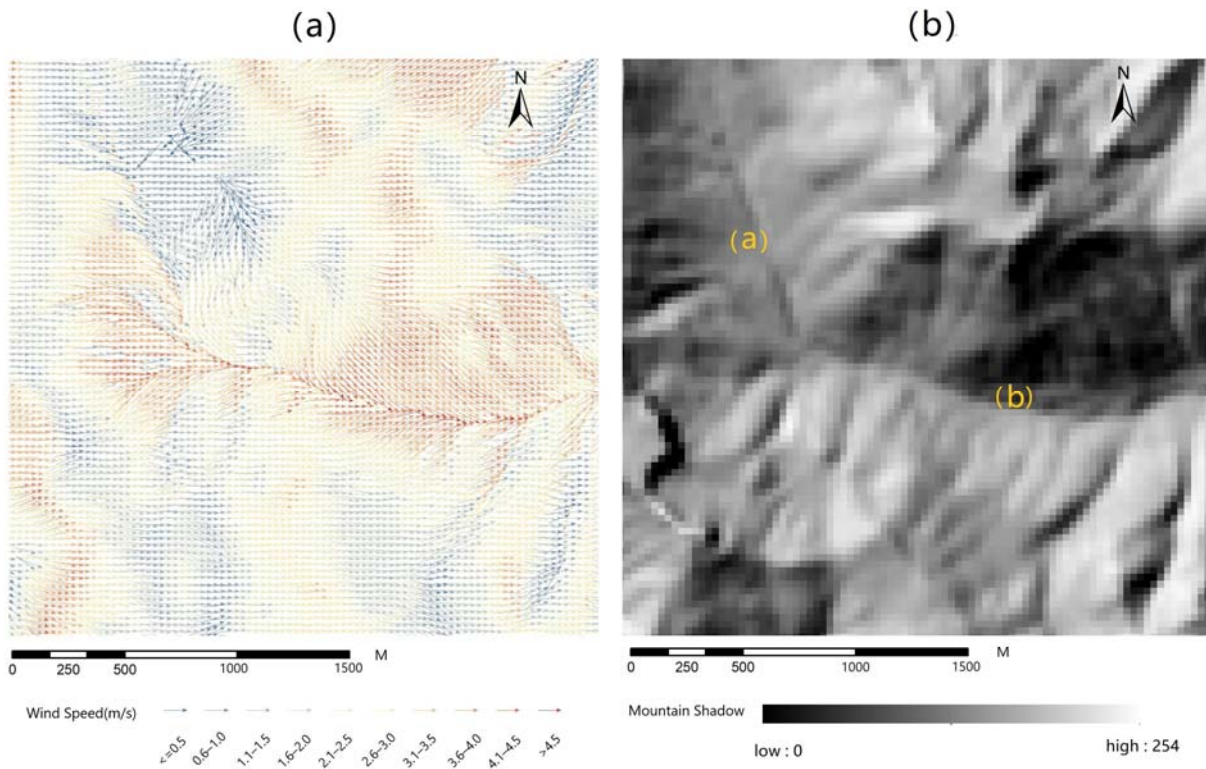


Fig. 3 Wind speed and direction in typical valley areas in the study area: (a) Wind speed and direction; (b) Topography represented by shading of mountains

(2) Influence of Ridge Topography on Wind Field Variation

As shown in Fig. 4, there are two types of ridges in this region, (a) and (b), with ridge (a) approximately parallel to the wind field direction and ridge (b) approximately perpendicular to the wind field direction. It can be observed that there is no significant change in wind speed and wind direction when turbulence passes through ridges (a1), (a2), and (a3), but there is a significant increase in wind speed when it reaches the position of ridges (b1) and (b2), with different increases at

different positions. It can be concluded that in the ridge area, when the wind field direction is parallel or nearly parallel to the valley direction, the wind direction and wind speed passing through the ridge will not show obvious changes; while when the wind field direction is perpendicular or nearly perpendicular to the ridge direction, the wind speed will increase when the turbulence reaches the ridge position, and the rate and magnitude of the speed increase is related to the steepness of the ridge.

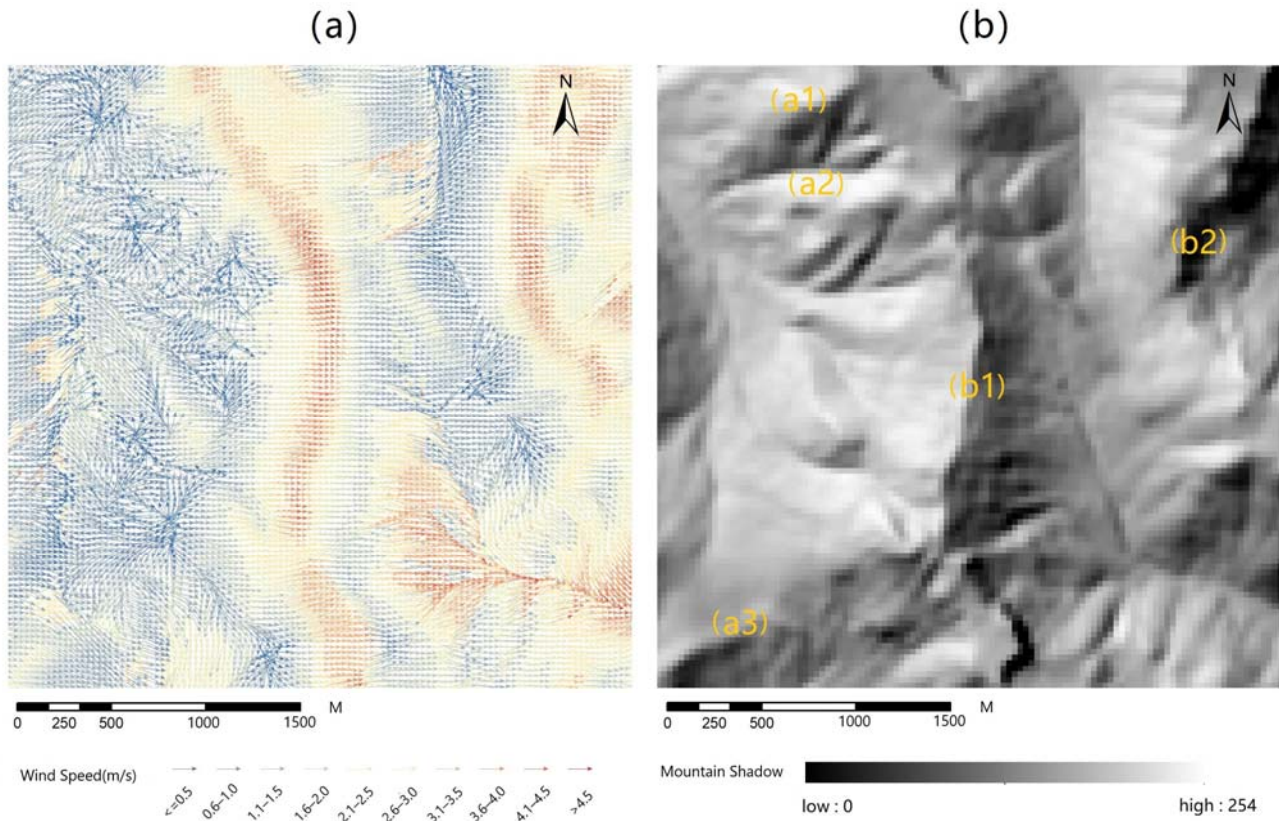


Fig. 4 Wind speed and direction in typical ridge areas in the study area: (a) Wind speed and direction; (b) Topography represented by shading of mountains

IV. SIMULATION AND ANALYSIS OF FOREST FIRE SPREAD DRIVEN BY FINE-GRAINED WIND FIELDS

A. Accuracy Verification

Based on the forest fire data recorded in the US historical fire dataset, the fire ELEVENMILE occurred on 24 August 2015, in the town of Custer, Idaho, covering an area of 114.504° W to 114.602° W and 44.426° N to 44.506° N, with a final burned area of approximately 10,724 acres. The historical fire vector data were overlaid with the fire data obtained from the final simulation of this study, and the results are shown in Fig. 5.

The final spread area of the simulated forest fire was calculated to be 13,113 acres, and the overestimated area was 2389 acres compared with the actual spread area. By superimposing the two vectors, it can be observed that in the upper right and lower left areas, the spread area of the simulated results was similar to the spread trend of the historical real data,

although the simulated fire area in the lower area was larger compared with the actual fire area. Despite this, from the overall data analysis, the area where the real and simulated burn overlaps was 10,209 acres, accounting for 95.20% of the real value and 77.85% of the simulated value, so it can be said that the spread simulation of this study was realistic for this area.

B. Results and Analysis

1. Total Process Spread Growth Area and Rate

Fig. 6 shows the change of fire spread area day by day from 24 August to 29 August, and Fig. 7 shows the growth rate of fire spread area hour by hour from 24 August at 00:00 to 29 August at 23:00. The analysis shows that the fire spread rate was at its maximum in the hours when the fire initially started to spread, and gradually decreased with time. In the total spreading time of 141 h, the spreading rate decreased sharply in the first 24 h and reached a more stable spreading state after 24

h. In the last day of the simulation, i.e., 29 August, a fast growth rate occurred at 12:00, with a growth rate of 3.49%, while the

average daily growth rate was 1.64%. At this point the spread was close to termination, and we stopped the simulation.

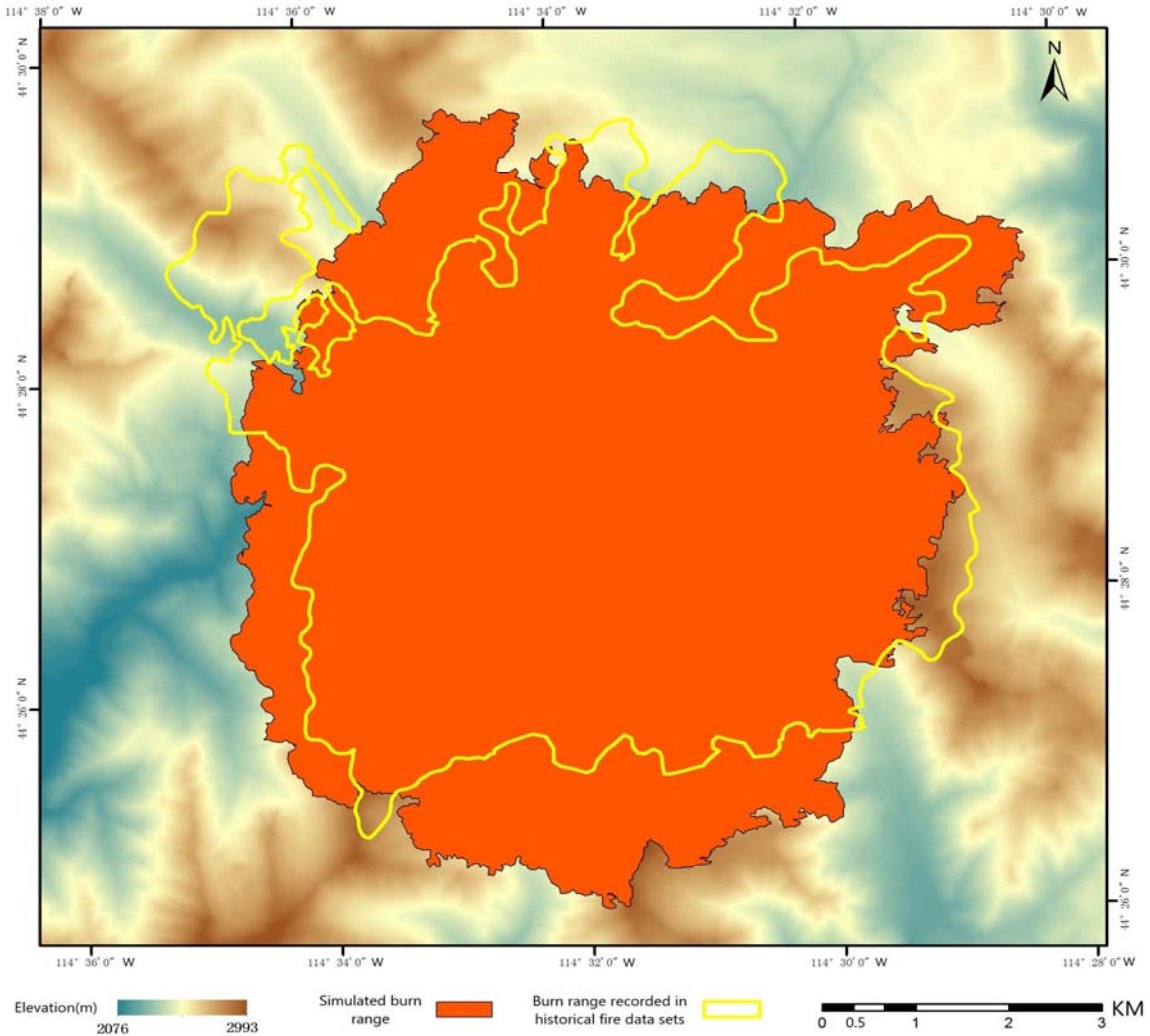


Fig. 5 Comparison of simulated fire spread range and historical actual burning range

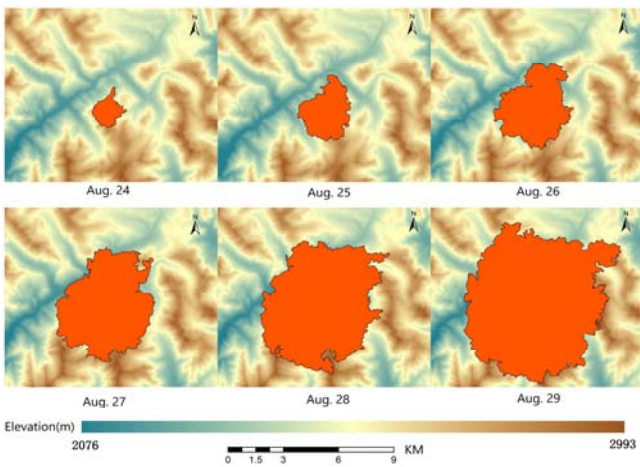


Fig. 6 Simulation results of daily fire spread from 24 August to 29 August

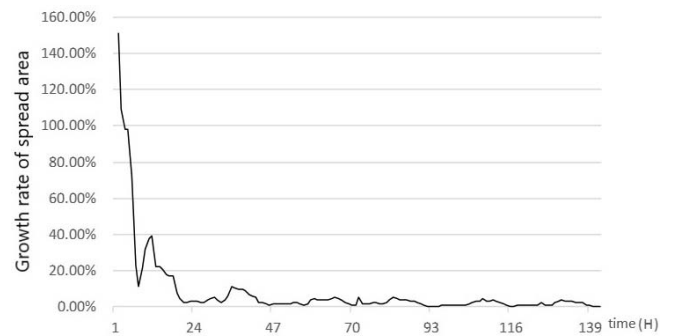


Fig. 7 Hourly fire spreading area growth rate from 0:00 on 24 August to 23:00 on 29 August

2. Fire Spread Growth Area with the Wind Field

To observe more clearly the small changes in fire spread after 24 h, the simulation results from 24 August were removed and retabulated in this study, and the hourly average wind speed was

combined with the analysis to obtain the wind speed and weighted fire spread area changes over time, as in Fig. 8.
 Based on this rule, the correlation analysis between the fire spread growth area and wind speed simulation results from 25 August at 00:00 to 29 August at 23:00 and the linear regression

model were established to obtain a scatter plot of the correlation between the fire spread growth area and wind speed, as shown in Fig. 9. The model correlation and parameter estimation values are given in Table V.

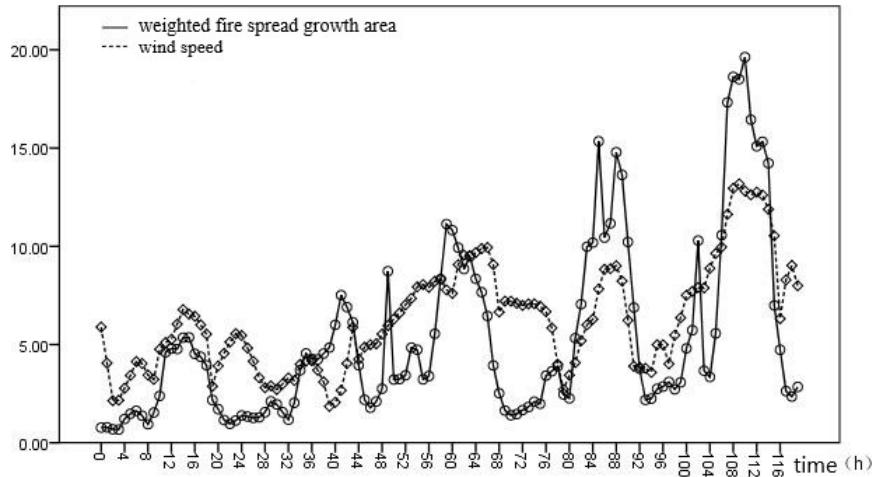


Fig. 8 Wind speed and weighted fire spread growth area change with time

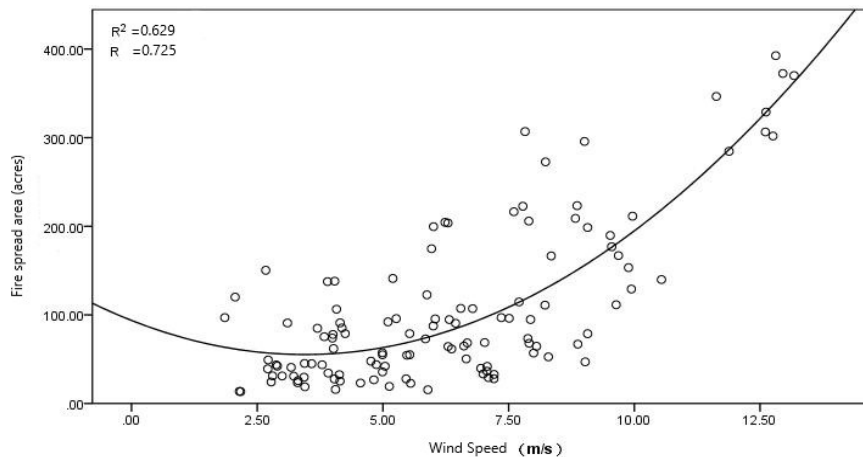


Fig. 9 Scatter plot of the correlation between the fire spread area and wind speed

MODEL CORRELATION AND PARAMETER ESTIMATES	
Model Correlation	Parameter Estimates
$R^2 = 0.629$	Constants = 93.761 b1 = -22.353 b2 = 3.247

From Fig. 9 and Table V, it can be seen that in this period (25 August at 00:00 to 29 August at 23:00), the correlation R^2 value between the fire spread growth area and wind speed was 0.629, and the correlation coefficient was 0.725, which means that after the fire burned and spread, then reached the steady-state, the fire spread growth area began to be significantly positively correlated with the wind speed. The correlation between the spread area (S) and wind speed (V) can be expressed according to the modeling results, as follows:

$$S = 3.247V^2 - 22.353V + 93.761 \quad (4)$$

This significant positive correlation demonstrates that more accurate simulation results can be achieved by using fine-grid winds to simulate fire spread in small areas.

3. The Relationship between the Change in Fire Spread Rate and the Change in Slope

As shown in Fig. 10, the wind speed and direction in the study area did not change significantly during this period, but the fire head growth in position ①, ③ was significantly faster than that in position ②, and the slope in position ①, ③ was also significantly larger than that in position ②, which proves that the change of slope significantly changed the fire spread rate during the spreading process, and they are positively correlated. The slope correction coefficient in the Rothermel model used in this paper, as the numerator term in the equation, was significantly and positively correlated with the fire spread rate, which is consistent with the simulation results and justifies

the use of this model in the study area.

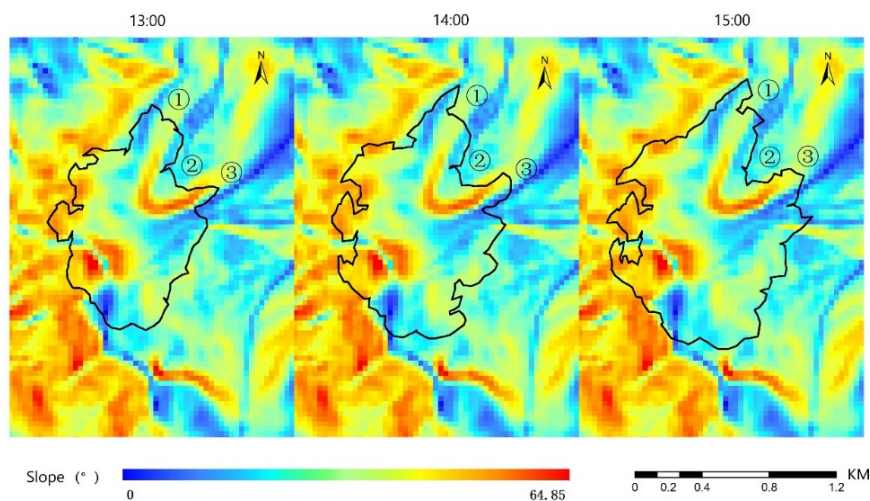


Fig. 10 Changes in the area of fire spread from 13:00 to 15:00 on 24 August

V. CONCLUSIONS AND PROSPECTS

A. Conclusions

1. In this paper, numerical simulations of fine wind fields in mountainous areas were realized with high accuracy through the coupling of WRF and CFD. Based on the simulation results, we can conclude that the correlation between the wind speed simulation results and the measured data from meteorological stations was high, and the correlation coefficients were above 0.70, so the simulation results are reliable in terms of the wind speed variation trend. The correlation coefficients were above 0.79, and the accuracy of the wind simulation results was also high.
2. The influence of the topography on the mountain wind field is shown in the valley area of the small-scale mountain area. When the direction of the wind field is perpendicular or nearly perpendicular to the direction of the valley, the wind speed of the valley will decrease when it reaches the valley area. In the ridge area, when the wind field direction is parallel or approximately parallel to the valley direction, the wind direction and wind speed through the ridge will not show obvious changes; while when the wind field direction is perpendicular or approximately perpendicular to the ridge direction, the wind speed will increase when the turbulence reaches the ridge location, and the rate and magnitude of the increase are related to the steepness of the ridge.
3. Based on the Rothermel forest fire spread model and the FARSITE fire behavior simulation platform to realize the simulation of forest fire spread driven by a fine wind field in mountainous areas, the area where the real burn overlapped with the simulated burn was 10,209 acres, accounting for 95.20% of the simulated value and 77.85% of the real value. The simulation results have high credibility. The analysis of the fire spread trend concluded that the fire spreads fastest in the first few hours after the

initial start, and gradually steadies with time. The wind can greatly improve the simulation accuracy. The positive correlation of wind speed and slope with the fire spread rate also proved the rationality of using the Rothermel forest fire spread model in this study.

B. Prospects

Next, we need to understand more about the correspondence between vegetation cover and fuel data in different regions of China so that we can localize the model and apply the simulation method of this study to the simulation of forest fire spread in forest fire-prone areas in China, such as Liangshan Prefecture, in order to provide new ideas and methods for the simulation of forest fire spread in China and to support forest fire risk avoidance and rescue and relief in China in the future.

REFERENCES

- [1] Guo, T.; Zhou, Y. Forest fire and climate change. *For. Fire Prev.* 2015, 3, 34–37. (In Chinese)
- [2] Zhou, S. R.; He, C.; Chen, F.; Shu, L. F. Evaluation and analysis of forest fire hazards in China. *For. Fire Prev.* 2018, 2, 33–36. (In Chinese)
- [3] Zhu, J.J.; Zhou R.L.; Gao, J. J.; Long, T. T.; Shi, S. J.; Xu, B. D. Influence of slope on forest fire spread. *J. Agric. Catastrophol.* 2012, 2, 80–83. (In Chinese)
- [4] Hu, R.; Zhu, H. Forest fire occurrence factors and preventive technical measures. *Anhui Agric. Sci. Bull.* 2013, 19, 113–114. (In Chinese)
- [5] Zhang, S.; Zhu C.; Chen Z. Research on forest fire meteorological environmental elements and large forest fires. *J. Nat. Disasters* 2000, 2, 111–117. (In Chinese)
- [6] Li, L. Research on the Relationship between Forest Fires and Meteorological Factors in Yunnan Province; Beijing Forestry University: Beijing, China, 2010. (In Chinese)
- [7] Gemma, S.; Carlos, B.; Tomàs, M.; Cortés, A. Wind Field Uncertainty in Forest Fire Propagation Prediction. *Procedia Comput. Sci.* 2014, 29, 1535–1545.
- [8] Li, R. The Research on Influence of Wind for Fire Spread Real-time Changes. *Nat. Sci. J. Harbin Norm. Univ.* 2011, 27, 30–33.
- [9] Takanori, U.; Yuji, O. Micro-siting technique for wind turbine generators by using large-eddy simulation. *J. Wind. Eng. Ind. Aerodyn.* 2008, 96, 2121–2138.
- [10] Griffiths, A. D.; Middleton, J. H. Simulations of separated flow over two-dimensional hills. *J. Wind. Eng. Ind. Aerodyn.* 2009, 98, 155–160.
- [11] Zhang, J.; Cheng, X. Numerical Simulation of Wind Field in Complex

- Terrain based on CFD Downscaling. *Plateau Meteorol.* 2020, 39, 172–184.
- [12] Chen, X. Numerical Simulation Study of Wind Load on Complex Mountainous Wind Field and Angle Steel Transmission Tower; Hefei University of Technology: Hefei, China, 2017.
- [13] Pan, T. Simulation of Atmospheric Boundary Layer Wind Field Based on OpenFOAM; Chongqing University: Chongqing, China, 2015.
- [14] Frandsen, W.H.; Rothermel, R.C. Measuring the Energy-Release Rate of a Spreading Fire; Elsevier: Amsterdam, The Netherlands, 1972; Volume 19.
- [15] Butler, B.W.; Wagenbrenner, N.S.; Forthofer, J.M.; Lamb, B.K.; Shannon, K.S.; Finn, D.; Eckman, R.M.; Clawson, K.; Bradshaw, L.; Sopko, P.; Beard, S.; et al. High-resolution observations of the near-surface wind field over an isolated mountain and in a steep river canyon. *Atmos. Chem. Phys.* 2015, 15, 3785–3801.
- [16] Prieto-Herráez, D.; Frías-Paredes, L.; Cascón, J.M.; Lagüela-López, S.; Gastón-Romeo, M.; Asensio-Sevilla, M.I.; Martín-Nieto, I.; Fernandes-Correia, P.M.; Laiz-Alonso, P.; Carrasco-Díaz, O.F.; et al. Local wind speed forecasting based on WRF-HDWind coupling. *Atmos. Res.* 2020, 248, 105219.
- [17] Zhao, L.; Liu, P.; Zhou, Y.; Shi, J.; Tang, M. Wind field interpolation over complex terrain and its application in the simulation of forest fire spreading. *J. Beijing For. Univ.* 2010, 32, 12–16.
- [18] Hong, S.; Lim, J. The WRF Single-Moment 6-Class Microphysics Scheme (WSM6). *Asia-Pac. J. Atmos. Sci.* 2006, 42, 129–151.
- [19] Rolf-Erik, K.; Niklas, S. Validation of uncertainty reduction by using multiple transfer locations for WRF–CFD coupling in numerical wind energy assessments. *Wind. Energy Sci.* 2020, 5, 997–1005.
- [20] Yang, Y.; Tan, J. C.; Jin, B. C.; Liu, M. G. Multi-Scale Simulation on the Wind Field for Complex Terrain Based on Coupled WRF and CFD Techniques. *J. South China Univ. Technol.* 2021, 49, 65–73, 83.
- [21] Zachary, J.L.; Andrea, B. A 14,000-year record of fire, climate, and vegetation from the Bear River Range, southeast Idaho, USA. *Holocene* 2016, 26. <https://doi.org/10.1177/0959683615622545>.
- [22] Cathy, W.; Christy, E.B.; Matias, C.F.; Gage, J. Holocene vegetation, fire and climate history of the Sawtooth Range, central Idaho, USA. *Quat. Res.* 2011, 75, 114–124.
- [23] Natalie, S.W.; Jason, M.F.; Wesley, G.P.; Butler, B. Development and Evaluation of a Reynolds-Averaged Navier–Stokes Solver in Wind Ninja for Operational Wildland Fire Applications. *Atmosphere* 2019, 10, 672.
- [24] Li, C. CFD Simulation Study of Turbulent Wind Field near the Ground; Harbin Institute of Technology: Harbin, China, 2010.
- [25] Michal, F.; Július, P. Existence of solution of a forest fire spread model. *Appl. Math. Lett.* 2018, 83, 227–231.
- [26] Zhu, L. Forest fire simulation comparison based on Wang Zhengfei model and Rothermel model. *Agric. Sci.-Technol. Inf.* 2019, 3, 85–88.
- [27] Yang, S.; Li, N. Advances in Forest Fire Spread Models. *Gansu Sci. Technol.* 2021, 37, 45–47.